Anthropogenic changes of the thermal and zonal flow structure over Western Europe and Eastern North Atlantic in CMIP3 and CMIP5 models

Reindert J. Haarsma, Frank Selten and Geert Jan van Oldenborgh

Royal Netherlands Meteorological Institute

Corresponding author:

Reindert J. Haarsma
Royal Netherlands Meteorological Institute (KNMI)
P.O. Box 201
3730 AE De Bilt
The Netherlands
haarsma@knmi.nl
Tel: +31 30 2206768

July 2012

Submitted to Climate Dynamics

Abstract

The anthropogenic changes in the thermal and zonal flow structure over Eastern Atlantic and Western Europe have been investigated using an ensemble of CMIP3 and CMIP5 models. The ensemble mean change in the zonal wind at 500 hPa over eastern Atlantic and Western Europe (EAWE) is characterized by an eastward extension of the belt of zonal winds. Due to the thermal wind relation this is connected to changes in the tropospheric temperature profile characterized by a warming in the subtropical upper troposphere and a relative surface cooling in the mid-latitudes. The subtropical upper tropospheric warming is related to the downward branch of the mean meridional circulation, whereas the mid-latitude lower tropospheric relative cooling is caused by ocean processes that cool the surface. Differences in the simulated change of the zonal wind over the eastern Atlantic and Western Europe by the CMIP3 and CMIP5 models can to a large extend be related to differences in the upper tropospheric subtropical warming and the mid-latitude lower tropospheric relative cooling. Because of the large control of sea surface temperatures (SST) on the tropospheric temperature profile, the simulated change of the zonal wind over the EAWE region by the CMIP3 and CMIP5 models can also to a large extend be related to the meridional SST gradient.

1 Introduction

The regional impact of climate change is to a large extent governed by the change in the atmospheric circulation. Van Ulden and van Oldenborgh (2006) demonstrated that the change in the strength of the westerly flow over Western Europe affects the temperature increase and change in rainfall over this area. This motivated the KNMI to use the change in the westerlies as a steering variable in their climate projections for the 21st century (Van den Hurk et al. 2007)

Anthropogenic widening of the Hadley circulation causes a poleward shift of the storm tracks and belt of zonal winds (Lu et al. 2007, 2009; Seidel et al. 2008; Yin 2005). However the regional differences simulated by the CMIP3 models (Meehl et al. 2007) are large as seen in Fig.1a showing the ensemble mean change for the boreal winter (DJF) in the 500 hPa zonal wind between 1971-2000 and 2071-2100 under an SRESA1B scenario. The models and the simulations that are used are described in Table I. Over Western Europe the main signal from the multi-model mean of CMIP3 models is an eastward extension of the belt of zonal winds instead of a pole ward shift as was also remarked by Lorenz and the Weaver (2007). In line with this Ulbrich et al. (2008) noted for the CMIP3 models a zonal extension of the storm track towards Europe. In other regions, such as the western Pacific, the pole ward shift of the subtropical jet is more clearly seen in Fig. 1a. The changes that are simulated by the recent CMIP5 models (http://cmip-pcmdi.llnl.gov/cmip5) for the RCP4.5 scenario (van Vuuren et al. 2011) that we have investigated here (Table II) are very similar in structure although slightly weaker (Fig. 1b). The latter is related to the smaller increase in greenhouse gases compared to the SRESA1B scenario. The strong similarity suggests that the same basic mechanisms are responsible for the simulated changes in the CMIP3 and CMIP5 models.

Woollings (2008) stressed the baroclinic structure of the anthropogenic response in the zonal flow. Over the Atlantic and surrounding regions large diabatic changes are simulated by the CMIP3 models in response to anthropogenic warming: a strong Arctic heating associated with radiative long-wave forcing, a relative cooling over the Northern Atlantic due to oceanic processes and a large tropical tropospheric heating caused by latent heat release (Intergovernmental Panel on Climate Change (IPCC) 2007). These strong diabatic heating sources will modify the tropospheric temperature profile. By means of the thermal wind relationship changes in the horizontal gradients of the temperature profile are associated with changes in the zonal wind profile. From the thermal wind balance by itself one cannot deduce the cause and effect relationship between the meridional thermal structure and the zonal wind profile. However, the change in the temperature structure due to anthropogenic climate change is primarily driven by the change in radiation due to the increase of greenhouse gases. The atmospheric circulation responds to these temperature changes in a consistent way. This adjustment can be so strong that locally the changes in the thermal structure are dominated by the changes in the wind profile. For the eastern Atlantic and Western Europe, however, we hypothesize that the diabatic contributions dominate the adiabatic contributions to the thermal changes. This hypothesis will be explored below.

2 Data and models

We have analyzed the output of the CMIP3 models using the SRES A1B scenario (Meehl et al. 2007). In addition we have also used the recent available CMIP5 (http://cmip-pcmdi.llnl.gov/cmip5) (Taylor et al. 2012) models with the RCP4.5 (van Vuuren et al. 2011) scenario. The CMIP3 models and the simulations that are used are described in Table I. They are the same as used in Haarsma and Selten (2012). The CMIP5 models are described in Table II. We will refer to the periods 1971-2000 and 2071-2100 as Present and Future respectively. To give all CMIP3 and CMIP5 models the same weight we included only one member of each model in case more members were available.

In addition we have analyzed the climate change simulations of the ECHAM5/MPI-OMI model used in the ensemble experiment ESSENCE (Sterl et al. 2008). This is a 17 member ensemble also using the SRES A1B scenario. The large ensemble enables a clear separation between internal variability and the mean anthropogenic response. The code of ECHAM5/MPI-OMI model in ESSENCE is the same as the CMIP3 ECHAM5 model in Table I. Similar as for the CMIP3 and CMIP5 models we will refer to the periods 1971-2000 and 2071-2100 as Present and Future respectively.

With the climate model EC-EARTH (Hazeleger et al. 2010) we have performed experiments with prescribed SST which will be discussed more extensively below.

3 Results

3.1 Thermal wind balance

The thermal wind balance given by (1) is a dominant balance that results from combing the geostrophic and the hydrostatic equilibrium and holds well outside the tropical regions. It describes the change in wind with height in an atmospheric column due to the horizontal temperature gradient.

$$\vec{V}_T = \frac{R}{f} \ln\left[\frac{p_0}{p_1}\right] \vec{k} \times \nabla_p \overline{T} \qquad (1)$$

Here $\vec{V}_T$ is the thermal wind, $\overline{T}$ the mean temperature over the atmospheric column, ∇_p the horizontal nabla operator at constant pressure level, $\vec{k}$ the vertical unit vector, R the gas constant and f the coriolis parameter. p_0 and p_1 are the pressure at the surface and the top of the atmospheric column respectively: $p_0 > p_1$.

The thermal wind relationship is a powerful diagnostic tool and is recently been used by Allan and Sherwood (2008) to infer upper tropospheric warming in the tropical upper troposphere from changes in the zonal velocity as observed from radiosonde data over the last decades. Here we will use the thermal wind balance in the opposite direction: understanding the simulated changes in the wind field from the simulated changes in the temperature field. We will focus over the Eastern Atlantic, Western Europe (EAWE) region (15 ºW-15 ºE, 0-90 ºN), indicated by black lines in Fig. 1. This is for the CMIP3 and CMIP5 ensemble mean a region with large changes in the zonal wind over the northern North Atlantic (Fig. 1). It is also of great interest for Western Europe climate. Changes in the tropospheric zonal flow over this region strongly affect the surface climate (Van Ulden and van Oldenborgh 2006).

Figure 2a shows for the CMIP3 models the change in the zonally averaged temperature and zonal wind structure of EAWE. The zonal wind profile shows a maximum in the change of the zonal wind around 45 ºN that is consistent with the temperature change via the thermal wind balance. For the mid-latitudes this gradient is dominated by the tropical upper tropospheric warming around 30 ºN and the mid-latitude lower tropospheric reduced warming or relative cooling at about 55 ºN. The relevance of the thermal wind balance is illustrated in Fig. 2b showing the zonal wind profile computed from the thermal wind profile. It should be noted, however, that in the upward vertical integration of the meridional temperature distribution we prescribed as lower boundary condition the simulated change in the surface zonal wind. The more appropriate choice of downward vertical integration from the top of the atmosphere was not possible because of the low top of the CMIP3 models.

3.2 Origins of the change in the thermal structure over the Eastern Atlantic and Western Europe

In this section we will investigate the dynamical and physical causes of the change in the thermal structure in the EAWE region simulated by the CMIP3 models.

- *Upper tropospheric tropical heating with a downward extension around 20-30 ºN*

The tropical upper tropospheric heating seen in Fig. 2a is a common feature among CMIP3 and CMIP5 models (Intergovernmental Panel on Climate Change (IPCC) 2007). Recent studies indicate that this upper level warming is corroborated by the observations (Allan and Sherwood

2008). The tropical tropospheric heating extends in the EAWE region downward to the mid troposphere at about 25 ºN (Fig. 2). Figure 3a suggests that this heating is downward advected by the mean meridional circulation causing a band of enhanced temperatures at 500 hPa around 20-30 ºN. Especially over the Atlantic and Eurasia the climatological mean omega and anomalous temperature change have similar structure. This is underscored by the meridional structure of omega and temperature in the EAWE region (Fig. 3b). Significant differences between omega and the warming belt around 20-30 ºN, however, do exist, especially over the Pacific (Fig. 3a). Alternatively the warming at lower heights in the subtropical belt can be explained by the differences in relative humidity between the tropics and the subtropics and the associated temperature profiles. In the deep tropics the vertical temperature profile closely follows the wet-adiabatic profile, whereas in the subtropics it follows more the dry-adiabatic profile. The consequence is that uniform upper tropospheric warming in the tropics and subtropics will result in relatively warmer subtropics in the lower troposphere. In both explanations, however, the downward extension around 20-30 ºN is connected to the belt of subsidence in the present climate.

- *Mid-latitude lower tropospheric reduced warming*

Figure 3a reveals that the mid-lower tropospheric reduced warming seen in Fig. 2a appears to be part of a large scale mid-tropospheric reduced warming over the North Atlantic. A similar reduced warming or relative cooling is also apparent over the North Pacific. Over the Atlantic this mid-latitude relative cooling is associated with cold sea surface temperatures (SST) (Fig. 3c). The increase of the amplitude of the relative cooling from the mid- to lower-troposphere suggests that this relative cooling is generated by ocean processes. The relative cooling of the North Atlantic is a common feature of many CMIP3 models and is related to a weakening of the meridional overturning circulation (Intergovernmental Panel on Climate Change (IPCC) 2007). A similar relative cooling of SST is, however, not simulated for the North Pacific (Fig. 3c). This indicates that different mechanisms for the mid-tropospheric relative cooling over the two ocean basins are acting. Transient eddies contribute significantly to the momentum and heat balance in the storm track regions. Below we will investigate whether the differences between the Atlantic and Pacific basin can be ascribed to differences in the eddy activity between the two basins.

- *Role of eddy convergence terms*

It has been suggested that changes in eddy convergence play a major role in setting the storm track properties (Lu et al. 2009; Stephenson and Held 1993). We investigated whether this also holds for the EAWE region. The contribution of the transient eddies on the time mean heat balance is given by:

$$Q_E = -\left(\frac{1}{a\cos\varphi}\frac{\partial \overline{u'T'}}{\partial \lambda} + \frac{1}{a}\frac{\partial \overline{v'T'}}{\partial \varphi} + \frac{\partial \overline{\omega' T'}}{\partial p} - \frac{R}{pC_p}\overline{\omega' T'} - \overline{v'T'}\frac{\tan\varphi}{a} \right) \qquad (2)$$

whereas the eddy momentum convergence for the time mean zonal flow is given by:

$$F_{Ex} = -\left(\frac{1}{a\cos\varphi}\frac{\partial \overline{u'^2}}{\partial \lambda} + \frac{1}{a}\frac{\partial \overline{u'v'}}{\partial \varphi} + \frac{\partial \overline{u'\omega'}}{\partial p} - \frac{2\tan\varphi}{a}\overline{u'v'} \right) \qquad (3)$$

(Kok and Opsteegh 1985)

The prime variables are defined here as the deviations from the monthly mean values. The over bar denotes monthly mean. In the ESSENCE project the monthly mean values of UV, UT and VT were stored, from which the horizontal covariance terms can be computed (i.e. $\overline{UV} = \overline{U}\,\overline{V} + \overline{u'v'}$). The vertical covariance terms were not stored and are set to zero. The simulated changes of the wind and temperature profile of ESSENCE between Future and Present (Fig. 2c) are similar to those of the CMIP3 ensemble mean (Fig. 2a). This warrants the use of the ESSENCE eddy convergence terms to interpret the results of the CMIP3 models.

The change in Q_E and F_{Ex} between DJF Future and Present zonally averaged over the EAWE sector is shown in the upper panels of Fig. 4. For the thermal structure the sign of the contribution of eddies is opposed to the simulated changes: a cooling by the eddies of the subtropical warming, a warming in the mid-latitudes and a cooling in the Arctic. This reveals that transient eddies act to first order as a diffusive term to temperature anomalies. The contribution of the eddies to the zonal momentum balance of the EAWE sector is less clear but also generally diffusive. There are several studies that point to an important role for shaping the gradient in the zonal wind and that their impact on the momentum balance in the storm tracks is counter gradient (Lu et al. 2009; Stephenson and Held 1993; Lau et al. 1978). Indeed over the western Pacific (WP) storm track region (130-160 ºW) (indicated by black lines in Fig.1a) the eddies contribute significantly to the increase of the zonal wind between 40 and 50 ºN (Fig. 4 lower right panel). Similar as for the EAWA sector their contribution to the thermal balance is diffusive (Fig. 4 lower left panel).

We conclude that for the EAWE region the transient eddies do modify the temperature and zonal wind structure but that their role is mainly diffusive, opposing the anomalies. For the Pacific the situation is different. There the eddies significantly contribute to the change in the wind field. Because of the thermal wind balance this also indicates that the meridional temperature gradient is increased by the eddy activity. Thus the mid-tropospheric cooling over the Pacific appears to be partly generated by the change in the eddy activity.

3.3 Connection of the dominant changes in the temperature pattern with those in the wind pattern

To further investigate the relation between the westerlies in the EAWE region and the dominant structures in the temperature pattern in the CMIP3 models we linearly the maximum wind speed at 500 hPa between 40-60 ºN on the difference between the temperature averaged between 25-35 ºN at 400 hPa and SST averaged over the area (60-65 ºN, 30 ºW-5 ºE). We have taken the maximum wind between 40-60 ºN because, depending on the details of the temperature pattern, the location of the maximum wind shifts with the latitude. The results are shown in Fig. 5. It reveals a good correlation (r=0.74, which with 13 data points is significant at the 99.5% confidence level) indicating that the change in the intensity of the increase of westerlies over Western Europe simulated by the CMIP3 models is to a large extend determined by the change in the temperature difference between the subtropical upper tropospheric heating and the sub-polar surface cooling.

3.4 Understanding the differences between the CMIP3 models

Most CMIP3 models show an increase of zonal winds of Western Europe. However, significant differences between the different CMIP3 models exist as shown in Fig. 5. We will investigate here two models: one model that has a strong increase in the zonal wind between 40-60 ºN (GFDL21) and one model that has hardly any change in the zonal wind (MIROCHI). Figure 6ab shows for both models for the EAWE region the zonally averaged temperature and wind profile. The strong increase of the zonal wind in GFDL21 is related to strong increase of the north-south temperature gradient in the upper troposphere, whereas the MIROCHI is characterized by the absence of an increase in the meridional temperature gradient. Another salient difference between GFDL21 and MIROCHI is the much larger increase in tropospheric temperatures in MIROCHI. The warmer troposphere in MIROCHI compared to GFDL21 is also reflected by higher SSTs (Fig. 6cd). However, the change in SST is much more homogeneous than in GFDL21, which actually shows a cooling near Greenland associated with a decrease in strength of the Atlantic meridional overturning circulation.

To investigate the connection of the change in SST with the change in the tropospheric temperature and wind profile we have forced EC-EARTH with the SST fields of GFDL21 and MIROCHI respectively. This was done for the Present as well as the Future climate. The sea-ice concentrations were also taken from both models. The greenhouse concentrations were set according to the SRESA1B scenario. The duration of the simulations was 50 year. The results are averaged over the last 40 years. Figures 6e and 6f show the temperature and wind profiles between Future and Present of EC-EARTH forced with GFDL21 and MIROCHI SST respectively. A comparison between Fig. 6ef and 6cd reveals large similarities in those profiles. Both figures show the reduced tropospheric warming due to cold subpolar SSTs and the tropical upper tropospheric heating with its downward extension in the subtropics. Forcing EC-EARTH with the SST of GFD21 and MIROCHI also recaptures to a large extend the differences between those models. The strong tropospheric temperature response to the SST forcing is primarily due to the water vapor feedback (Schneider et al. 2010). We should note, however, that the SST forced experiment is an 'unrealistic' experiment in the sense that the ocean is treated as an infinite source of heat. The correct interpretation is not that the tropospheric temperature profile is forced by SST in a coupled climate simulation but that we can reconstruct the tropospheric temperature profile by forcing an atmospheric model with the SST of the coupled climate (Bretherton and Battisti 2000). Due to the close connection between the temperature and wind profile also the wind pattern is to a large extend reconstructed, with strong westerlies between 50-60 ºN for the GFDL21 SST and much weaker westerlies for the MIROCHI SST.

3.5 Connection between changes in SST and wind pattern

Because of the strong impact of the SST fields on the tropospheric temperature profiles it is natural to ask, based on the results shown in Fig. 6, whether there is also a relationship between SST and the westerlies over Europe. As discussed in section 3.2, the subtropical upper tropospheric temperatures are probably caused by downward advection of tropical upper tropospheric heat. The tropical upper tropospheric heat is related to tropical SST as discussed in section 3.4. We therefore redid the regression of Fig. 5 but now with the subtropical upper tropospheric temperatures replaced with the tropical Atlantic SST (0-15 ºN, 30-0 ºW). The results, displayed in Fig. 7a, are similar to Fig. 5 with a correlation of 0.71. This indicates that the increase of westerlies over Europe in a warmer climate is associated with the enhanced SST gradient over the Atlantic between the tropics and the subpolar gyre. The differences between the dynamical responses of the CMIP3 models are related to the differences in the simulated SST gradient, which in this area is strongly influenced by the ocean circulation response.

3.6 CMIP5 models

Using 21 CMIP5 models (see table II), with the RCP 4.5 scenario we have independently tested the results obtained with the CMIP3 data set. As discussed in the introduction the ensemble mean change in the zonal wind over EAWE region is very similar to the CMIP3 change (Fig. 1b). In the last section it was shown for the CMIP3 models that the change in the maximum zonal wind in the EAWE region at 500 hPa is related to the change in the meridional SST gradient in the North Atlantic. For the CMIP5 models we have redone the regression of Fig.7a. The results are shown in Fig. 7b. The correlation is lower (r=0.56, which with 19 data points is significant at the 99.5% confidence level) but still indicates a significant impact of the meridional SST gradient on the zonal wind structure, thereby confirming the results of the CMIP3 models.

4 Conclusions and discussion

We have shown here that the changes in the zonal wind at 500 hPa over the eastern Atlantic and Western Europe (EAWE) are related to changes in the tropospheric thermal structure. Two processes appear to be important for the changes in the temperature profile: the upper tropospheric subtropical enhanced warming and the surface mid-latitude relative cooling. The relative strength of these processes modifies the meridional temperature gradient and consequently affects the zonal wind structure due to the thermal wind relationship. The subtropical upper tropospheric warming is related to the downward branch of the mean meridional circulation. The mid-latitude lower tropospheric relative cooling is caused by ocean processes that cool the surface. Differences in the simulated change of the zonal wind over the EAWE region by the CMIP3 models can to a large extend be related to differences in the upper tropospheric subtropical warming and the mid-latitude lower tropospheric relative cooling.

Experiments with prescribed SST indicate that the SST exerts a large control over the tropospheric temperature profile. Indeed the simulated change of the zonal wind over the EAWE region by the CMIP3 models can also to a large extend be related to the meridional SST gradient. This result is confirmed by an independent set of CMIP5 models.

The contribution of the transient eddies to the zonal momentum and thermal balance appears to be minor over the EAWE region. This is different for the storm track region in the western Pacific. There the transient eddies do play a significant role in the momentum budget. In particular they are partly responsible for the increase of the zonal flow as simulated by the ensemble mean of the CMIP3 models. Because of the thermal wind relationship the simulated changes in the thermal wind structure in this region are also to large part associated with dynamical changes. The mid-latitude cooling in the Western Pacific is not due to surface cooling as in the eastern Atlantic, but related to the enhanced zonal wind induced by the transient eddies.

The fundamental difference in the role of the transient eddies between the eastern Atlantic and western Pacific is the different eddy activity in these two regions. The western Pacific region is located in the maximum of the storm track region whereas the EAWE region is situated downstream of the Atlantic storm tracks with significant less baroclinic activity.

Another significant difference is the ocean circulation. In the Atlantic changes in the meridional overturning circulation (MOC) significantly affect the SST distribution and subsequently the zonal wind in a future climate. A similar mechanism is absent in the Pacific.

The physical processes responsible for the changes in the simulated zonal wind profile appear to be regionally dependent. For the EAWE region we have identified these processes and shown that they are related to diabatic processes affecting the meridional thermal wind profile. Our results are supported by Woollings et al. (2012) who show that the strengthening and eastward extension of the North Atlantic storm track is related to the weakening of the MOC.

5 References

Allen RJ, Sherwood SC (2008) Warming in the upper tropical troposphere deduced from thermal winds. Nature Geo Sci 1:399-403

Bretherton CS, Battisti DS (2000) An interpretation of the results from atmospheric circulation models forced by the time history of observed sea surface temperature distribution. Geophys Res Lett 27:767-770

Haarma RJ, Selten FM (2012) Anthropogenic changes in the Walker Circulation and their impact on the extra-tropical planetary wave structure in the Northern Hemisphere. Clim Dyn Early online doi: 10.1007/s00382-012-1308-1

Hazeleger W, Severijns C, Semmler T, Stefanescu S, Yang S, Wang X, Wyser K, Dutra E, Bintanja R, van den Hurk B, van Noije T, Selten F, Sterl A (2010) EC-Earth: A Seamless Earth-System Prediction Approach in Action. Bull Amer Meteor Soc 91:1357-1363

Intergovernmental Panel on Climate Change (IPCC) (2007) The Physical Science Basis, edited by S. Solomon et al., Cambridge Univ. Press, Cambridge, UK.

Kok CJ, Opsteegh JD (1985) Possible causes of anomalies in seasonal mean circulation patterns during the 1982-83 El Niño event. J Atmos Sci 42:677-694

Lau N-C, Tennekes H, Wallace JM (1978) Maintenance of the momentum flux by transient eddies in the upper troposphere. J Atmos Sci 35:139-146

Lorenz DJ, DeWeaver ET (2007) Tropopause height and zonal wind response to global warming in the IPCC scenario integrations. J Geophys Res 112:D10119, doi:10.1029/2006JD008087

Lu J, Vecchi GA, Reichler T (2007) Expansion of the Hadley cell under global warming. Geophys Res Lett 34:L06805. doi:10.1029/2006GL028443

Lu J, Deser C, Reichler T (2009) Cause of the widening of the tropical belt since 1958. Geophys Res Lett 36: L03803. doi:10.1029/2008GL036076

Meehl G, Covey C, Delworth T, Latif M, McAveney B, Mitchell J, Stouffer R, Taylor K (2007) The WCRP CMIP3 multimodel dataset. Bull Am Met Soc 88:1383-1394

Seidel DJ, Fu Q, Randel WJ, Reichler TJ (2008) Widening of the tropical belt in a changing climate. Nat Geo Sci 1:21– 24

SchneiderT, O'Gorman PA, Levine XJ (2010) Water vapor and the dynamics of climate changes. Rev Geophys 48:RG3001. doi:10.1029/2009RG000302

Stephenson DB, Held IM (1993) GCM response of northern winter stationary waves and storm tracks to increasing amounts of carbon dioxide. J Clim 6:1859–1870

Sterl A, Severijns C, Dijkstra H, Hazeleger W, van Oldenborgh GJ, van den Broeke M, Burgers G, van den Hurk B, van Leeuwen PJ, van Velthoven P (2008) When can we expect extremely high surface temperatures? Geophys Res Lett. 35:L14703. doi:10.1029/2008GL034071

Taylor KE, Stouffer RJ, Meehl GA (2012) An overview of CMIP5 and the experimental design. Bull Amer Meteor Soc 93:485-498

Van den Hurk BJJM., Klein Tank AMG, Lenderink G, van Ulden A, van Oldenborh GJ, Katsman C, van den Brink H, Keller F, Bessembinder J, Burgers G, Komen G, Hazeleger W, Drijfhout SS (2007) New Climate scenarios for the Netherlands, Water Science and Technology. 56: 27-33. doi : 10.2166/wst.2007.533

Ulbrich U, Pinto JG, Kupfer H, Leckebusch GC, Spangehl T, Reyers M (2008) Changing Northern Hemisphere Storm Tracks in an Ensemble of IPCC Climate Change Simulations. J Clim 21:1669-1679

Ulden AP van, van Oldenborgh GJ (2006) Large-scale atmospheric circulation biases and changes in global climate model simulations and their importance for climate change in Central Europe. Atmos Chem Phys 6:863–881

Vuuren van DP, Edmonds J, Kainuma M, Riahi K, Thomson A, Hibbard K, Hurtt G.C, Kram T. Krey V, Lamarque JF, Masui T, Meinshausen M, Nakicenovi N, Smith SJ, Rose SK (2011) The representative concentration pathways: an overview. Clim Change 109:5-31

Woollings T (2008) Vertical structure of anthropogenic zonal-mean atmospheric circulation change, Geophy. Res Lett 35:L19702. doi:10.1029/2008GL034883

Woollings T, Gregory JM, Pinto JG, Reyers M, Brayshaw DJ (2012) Response of the North Atlantic storm track to climate change shaped by ocean–atmosphere coupling. Nature Geosci 5:313-317. doi:10.1038/ngeo1438

Yin, JH (2005) A consistent poleward shift of the storm tracks in simulations of 21st century climate. Geophys Res Lett 32:L18701. doi:10.1029/2005GL023684

Model name	Short name	Originating	Country	Atmospheric
CCSM3.1	CCSM3	NCAR	USA	T85,L26
CGCM3.1(T63)	CCCT63	CCCMA	Canada	T63,L31
CNRM-CM3	CNRM3	Met-France/ CNRM	France	T63L45
CSIRO-Mk3.0	CSIRO3	CSIRO	Australia	T63,L18
ECHAM5/MPI-OM	ECHAM5	MPI	Germany	T63,L31
GFDL-CM2.0	GFDL20	GFDL	USA	2.5x2,L24
GFDL-CM2.1	GFDL21	GFDL	USA	2.5x2,L24
INM-CM3.0	INM30	INM	Russia	5x4,L21
MIROC3.2(hires)	MIROCH	CCSR,NIES,FRCGC	Japan	T106,L56
MIROC3.2(medres)	MIROCM	CCSR,NIES,FRCGC	Japan	T42,L20
MRI-CGCM2.3.2	MRI	MRI	Japan	T42,L30
UKMO-HadCM3	HADCM3	UKMO	UK	3.75x2.5,L19
UKMO-HadGEM	HADGEM	UKMO	UK	1.875x1.25,L38

Table I CMIP3 models that have been analyzed.
More information is available online (http://www-pcmdi.llnl.gov)

Model name	Originating	Country
ACCES1-0	CAWCR	Australia
BCC_CSM1-1	BCC	China
CanESM2	CCCMA	Canada
CCSM4	NCAR	USA
CNRM-CM5	CNRM-CERFACS	France
CSIRO-MK3-6	CSIRO/QCCCE	Australia
GFDL-CM3	GFDL	USA
GFDL-ESM2G	GFDL	USA
GFDL-ESM2M	GFDL	USA
HadGEM2-ES	UKMO	UK
inmcm4	INM	Russia
IPSL-CM5A-LR	IPSL	France
IPSL-CM5A-MR	IPSL	France
MIROC5	MIROC	Japan
MPI-ESM-MR	MPI	Germany
MPI-ESM-LR	MPI	Germany
MRI-CGCM3	MRI	Japan
NorESM1-ME	NCC	Norway
NorESM1-M	NCC	Norway

Table II CMIP5 models that have been analyzed. More information is available online (http://cmip-pcmdi.llnl.gov/cmip5)

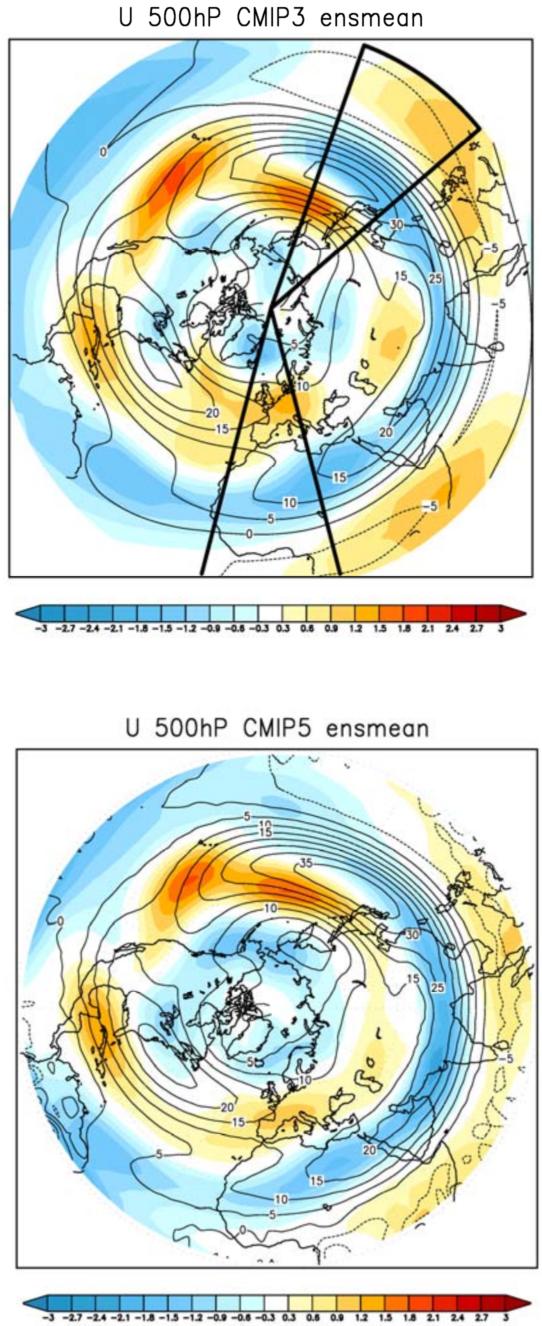

Fig. 1a Ensemble mean U (m s^{-1}) at 500 hPa for DJF simulated by the CMIP3 multi-model mean under the SRESA1B scenario. Contours: 1971-2000. Shaded: difference between 2071-2100 and 1971-2000. The solid black lines indicate the Eastern Atlantic, Western Europe (EAWE) region (0-90 ºN , 15 ºW – 15 ºE) and the Western Pacific region (WP) (0-90 ºN , 130 –160 ºW)
b. As **a** but now for the CMIP5 multi-model mean under RCP 4.5 scenario.

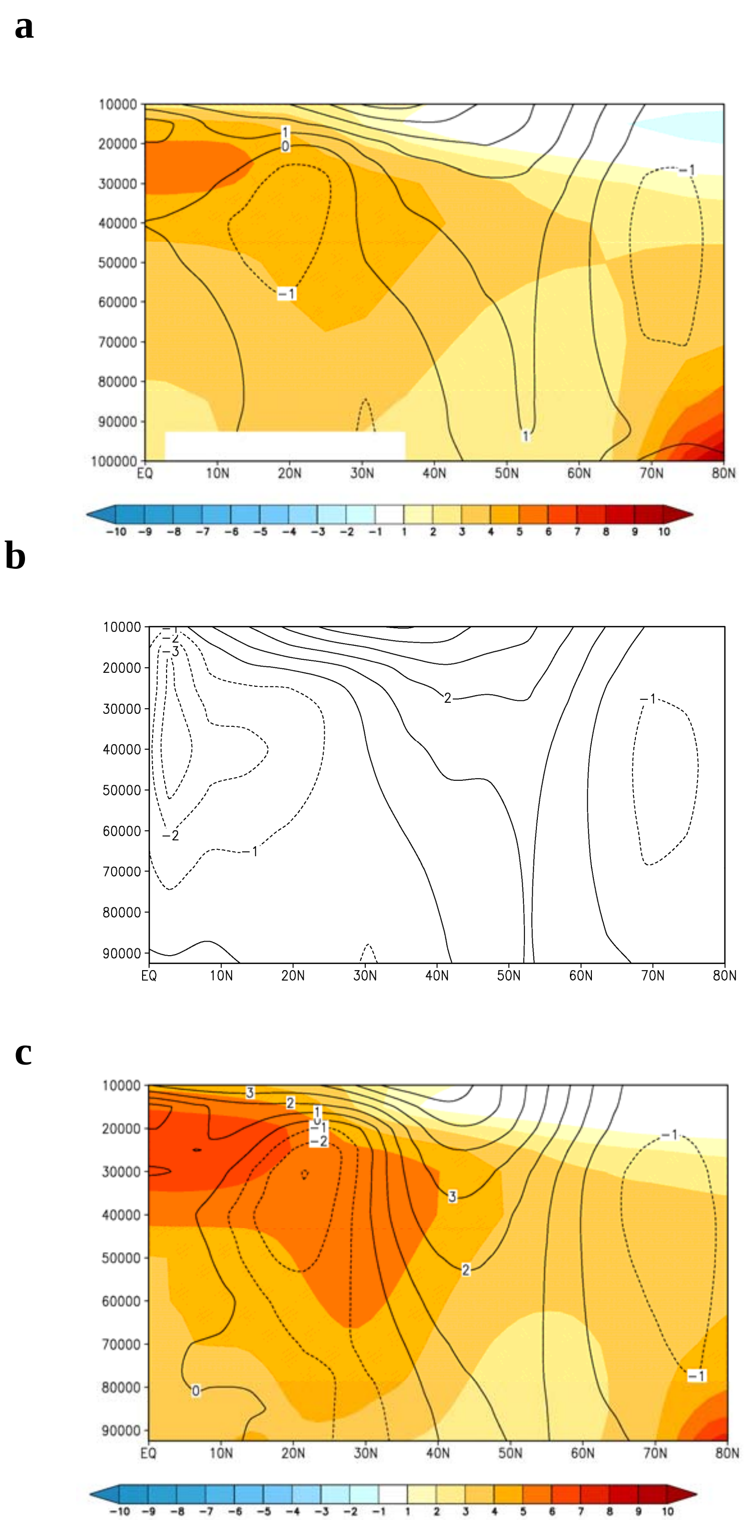

Fig. 2 a. CMIP3 ensemble mean difference for DJF between Future and Present zonally averaged over the region EAWE (15 ºW-15 ºE, 0 ºN-80 ºN), indicated by the black box in Fig.1.
Shaded: Temperature (K). Contours: U (m s^{-1}). Vertical axis in Pa.
b. Thermal wind (m s^{-1}) of CMIP3 ensemble mean computed from the temperature profile.
c. as **a.** but now for ESSENCE.

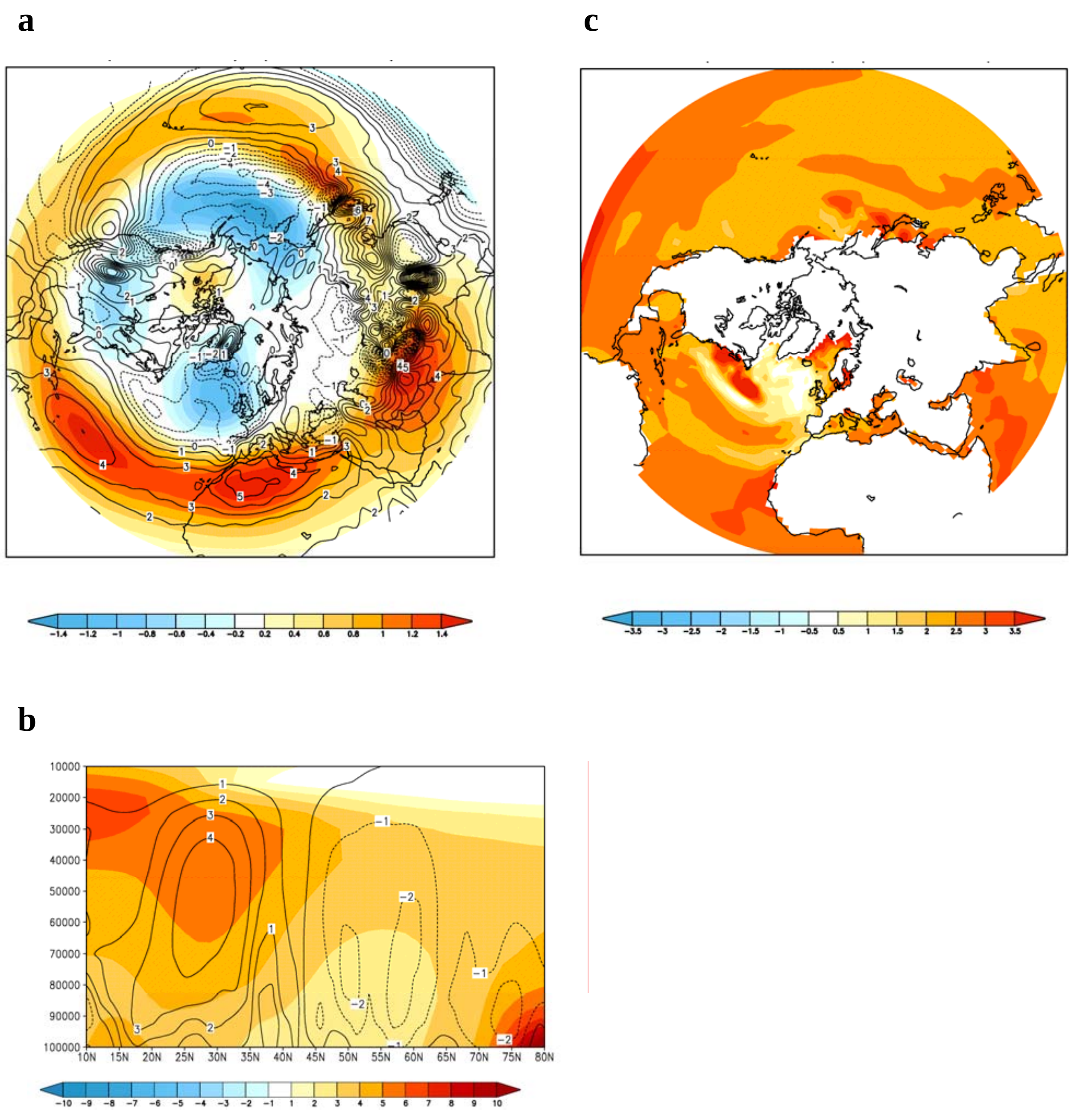

Fig. 3 Ensemble mean difference for DJF between Future and Present simulated by ESSENCE.
a: Temperature (shaded) at 500 hPa. To highlight the differences a continuous field of 4K has been subtracted. The contours are omega at 500 hPa (10^{-2} Pa s^{-1}) for the Present period.
b: Zonally averaged over the sector 10-80 ºN, 15 ºE-15 ºW. Shaded: temperature (K). Contours: omega (10^{-2} Pa s^{-1}).
c: SST (K)

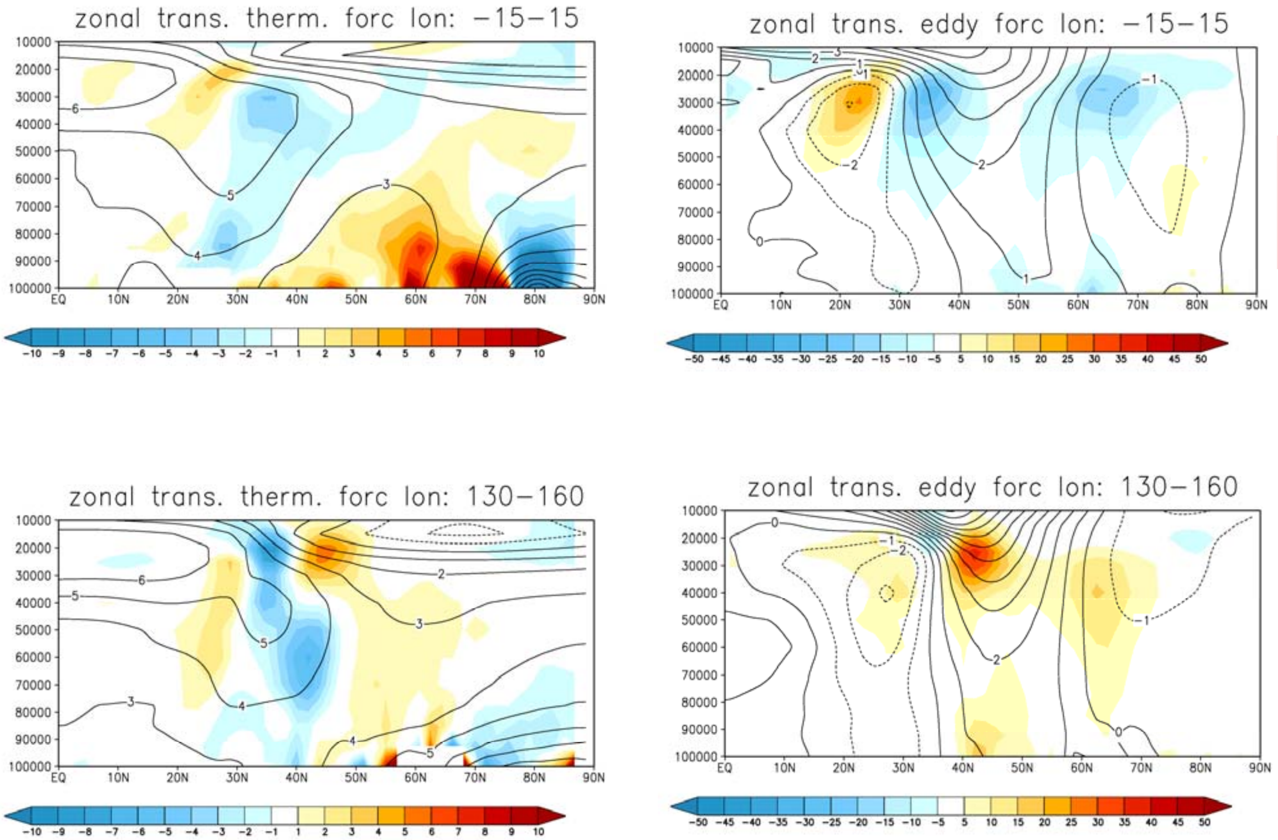

Fig. 4 Shaded: Change between Future and Present for DJF in ESSENCE of the eddy convergence terms in the thermal (left panels) (10^{-6} K s^{-1}) and momentum (right panels) (10^{-6} m s^{-2}) balance (See eqs. 2 and 3), zonally averaged for the Atlantic sector (15 ºW-15 ºE, 10-80 ºN) (upper panels) and the Western Pacific sector (130-160 ºW,10-80 ºN) (lower panels). The change in temperature (K) and zonal wind (m s^{-1}) are given by the solid contours.

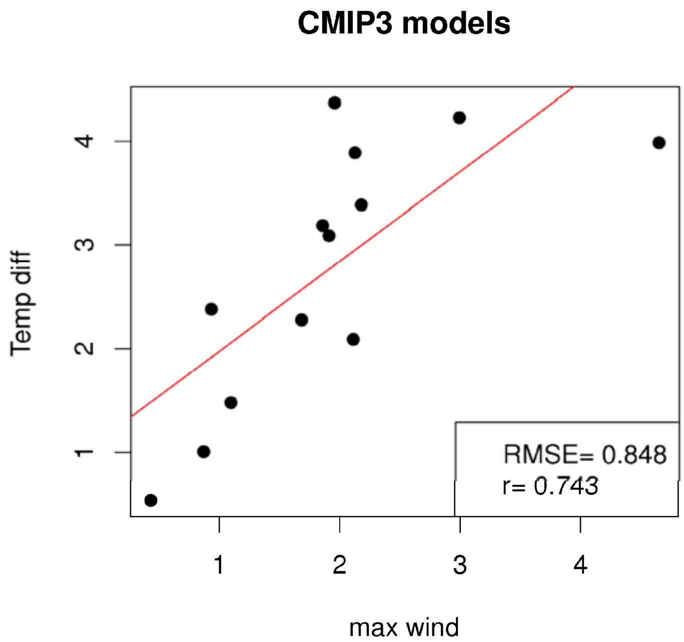

Fig. 5 Scatter plot of the CMIP3 models for DJF of the changes between Future and Present. Horizontal axis: maximum zonal wind (m s^{-1}) at 500 hPa zonally averaged over (15 ºW-15 ºE) between 30-70 ºN. Vertical axis: Difference between the temperature at 400 hPa averaged over the region (25-35 ºN; 15 ºW-15 ºE) and the SST averaged over the region (50-65 ºN, 45 ºW-5 ºE).

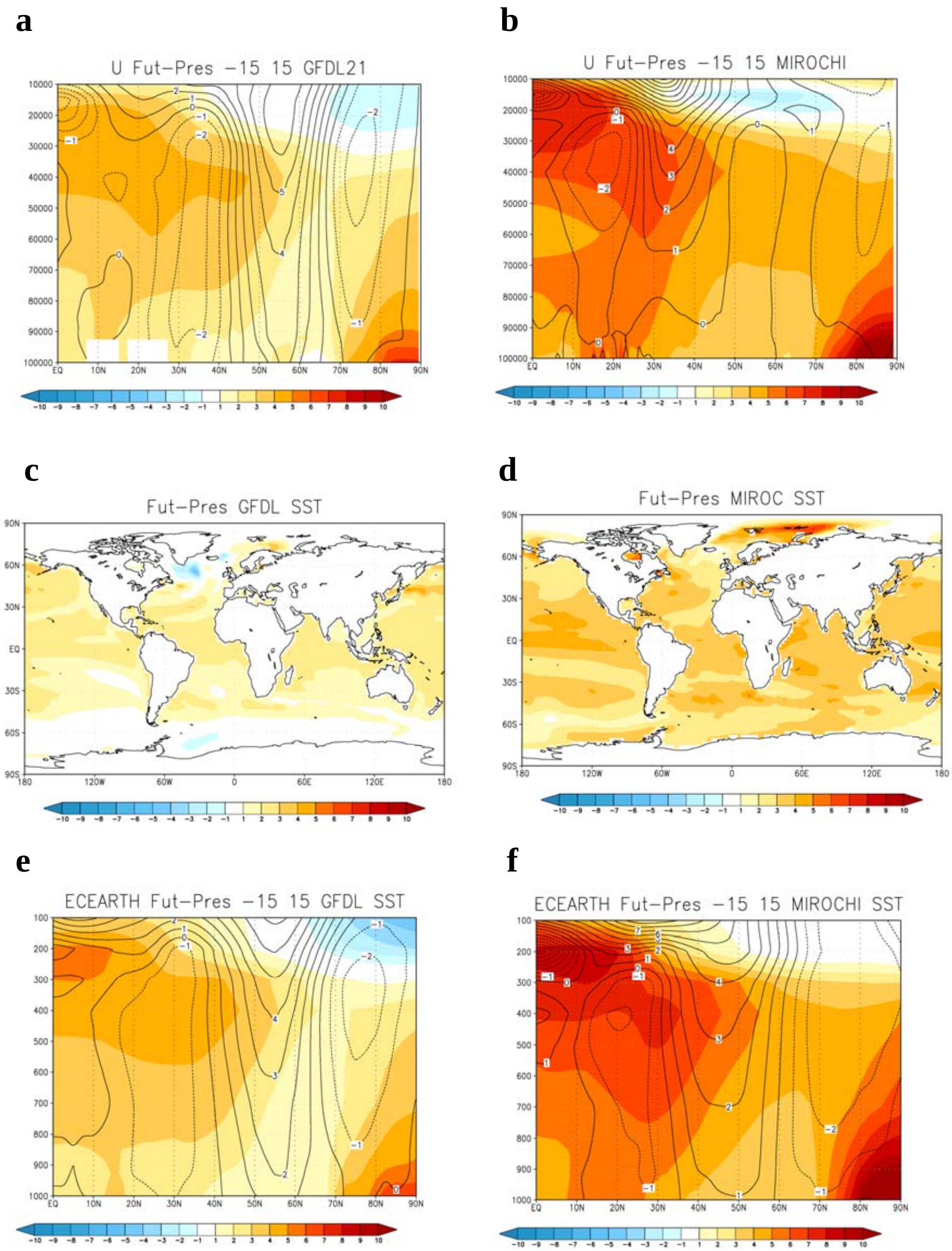

Fig. 6 Difference between Future and Present for DJF of simulated climate of GFDL21 (left panels) and MIROCHI (right panels).
Upper panels: temperature (shaded) (K) and zonal wind (contours) (m s^{-1}) zonally averaged over (15 ºW-15 ºE).
Middle panels: SST (K)
Lower Panels: temperature (shaded) (K) and zonal wind (contours) (m s^{-1}) zonally averaged over (15 ºW-15 ºE) of EC-EARTH forced with SST of GFDL21 (left) and MIROCH (right).

a

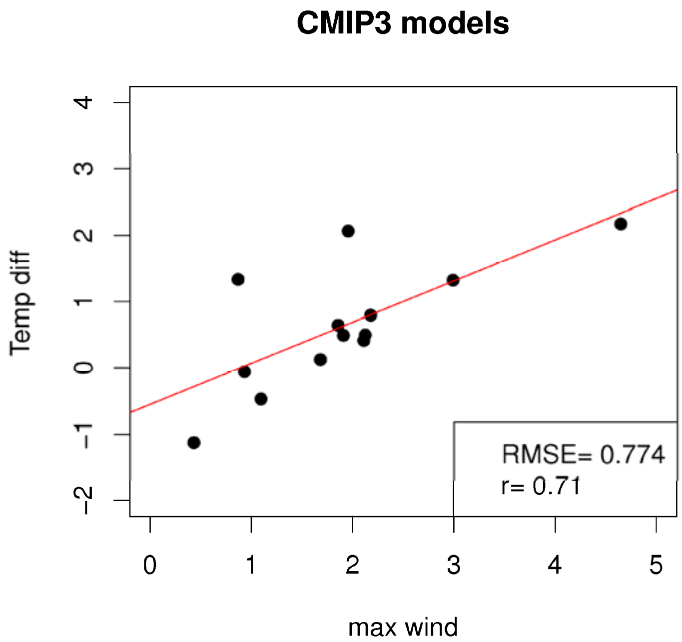

b

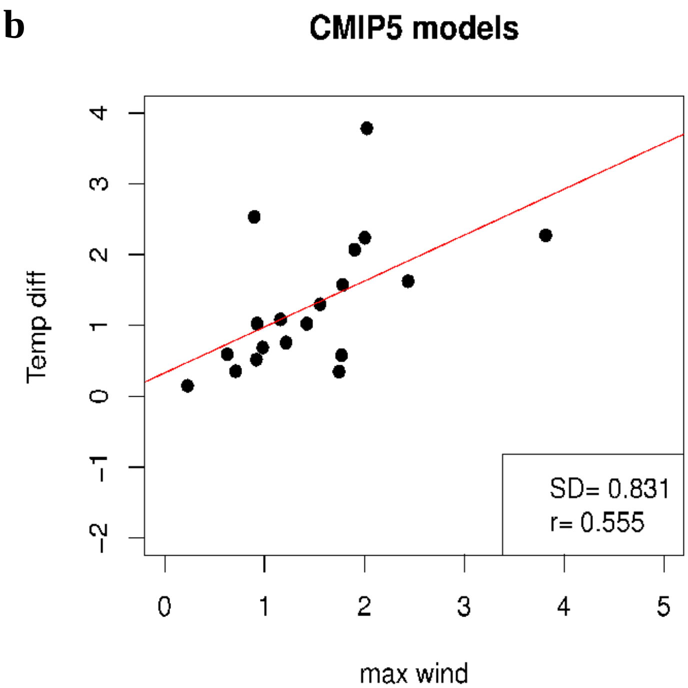

Fig. 7a Scatter plot of CMIP3 models of the changes between Future and Present for DJF. Horizontal axis: maximum zonal wind (m s^{-1}) at 500 hPa zonally averaged over (15 ºW-15 ºE) between 30-70 ºN. Vertical axis: Difference between SST (K) averaged over the region (0-15 ºN, 45-15 ºW) and (50-65 ºN, 45 ºW-5 ºE).
b as **a** but now for the CMIP5 models.